



3D-printed nanocarbon sensors for the detection of chlorophenols and nitrophenols: Towards environmental applications of additive manufacturing

Jyoti^a, Edurne Redondo^a, Osamah Alduhaish^{b,2}, Martin Pumera^{a,b,c,d,*},¹

^a Future Energy and Innovation Laboratory, Central European Institute of Technology, Brno University of Technology, Purkynova 123, Brno 61200, Czech Republic

^b Chemistry Department P. O. Box 2455, College of Science, King Saud University, Riyadh 11451, Saudi Arabia

^c Department of Chemistry and Biochemistry, Mendel University in Brno, Zemedelska 1, Brno 61300, Czech Republic

^d Department of Medical Research, China Medical University Hospital, China Medical University, No. 91 Hsueh-Shih Road, Taichung, Taiwan

ARTICLE INFO

Keywords:

3D-printed nanocarbon electrode
Phenols
Electrochemical analysis
Additive manufacturing

ABSTRACT

3D printing is a manufacturing technique used to prototype devices with customized shapes composed of different materials, including carbon composites. Toxic phenolic compounds are a major environmental hazard. Herein, we demonstrate the use of carbon-based 3D-printed electrodes for the detection of chlorophenols and nitrophenols. The influence of pH on the voltammetric response was studied, and an alkaline pH was identified as the best environment for the detection of substituted phenols. Simultaneous detection of phenolic compounds was performed using differential pulse voltammetry. This approach appears promising for the fabrication of electrochemical sensors.

1. Introduction

There is a considerable need to detect phenolic compounds in industrial, environmental, or food samples because of the toxicity of these compounds [1,2]. The conventional analytical methods used for detection, such as chromatography [3], capillary electrophoresis [4], and spectrophotometry [5] are time-consuming and the equipment is not portable. However, electrochemical methods have been shown to be suitable for rapid and portable detection of phenols and their substituents [6,7]. Various electrochemical analytical techniques (such as voltammetry) can be used for the facile electrochemical oxidation of phenols at a solid electrode, thus enabling their detection. Unfortunately, the electro-oxidation of these phenolic compounds produces phenoxy radicals, which combine to form a passivating layer at the electrode surface [1]. Considerable efforts have been made to identify new electrode materials and to develop a surface pre-treatment that would effectively avoid the surface fouling effects caused by the oxidation of phenols [8–10]. 3D printing of phenol-sensing platforms represents a promising approach, as the electrodes can be fabricated at

low cost. 3D printing, also known as additive manufacturing, is a recent technology that involves a layer-by-layer deposition process guided by computer-aided design (CAD) software [11]. This technique has many advantages compared to traditional electrode manufacturing techniques, including the rapid production of devices with minimal waste, high accuracy, good repeatability, high resolution, and high durability. Furthermore, it offers the possibility of customizing the shape and geometry of the produced object through a highly automated system with minimal human intervention [12,13]. In particular, the fused deposition modelling (FDM) printing technique can be utilized to fabricate 3D-printed nanocarbon electrodes (3DnCE): a composite filament consisting of thermoplastic polymer (polylactic acid (PLA)) and nanocarbon is extruded down the nozzle, and the desired shape is printed. Unfortunately, these surfaces have poor electrochemical activity due to the high amount of PLA needed for the successful extrusion and deposition of the materials. Hence, activation (some form of post-treatment) is needed to increase the electrochemical activity of the electrodes [14]. Thermal, electrochemical, and solvent treatments are among the most commonly used activation methods [15]. However, solvent treatment using *N,N*-

* Corresponding author at: Future Energy and Innovation Laboratory, Central European Institute of Technology, Brno University of Technology, Purkynova 123, Brno 61200, Czech Republic.

E-mail addresses: oaduhaish@ksu.edu.sa (O. Alduhaish), pumera.research@gmail.com (M. Pumera).

¹ orcid.org/0000-0001-5846-2951.

² orcid.org/0000-0001-5344-9459.

<https://doi.org/10.1016/j.elecom.2021.106984>

Received 30 December 2020; Received in revised form 4 February 2021; Accepted 14 February 2021

Available online 25 February 2021

1388-2481/© 2021 The Authors. Published by Elsevier B.V. This is an open access article under the CC BY license (<http://creativecommons.org/licenses/by/4.0/>).

dimethylformamide (DMF) is one of the simplest and fastest activation methods, providing an improved electrochemical response due to the removal of the PLA and the exposure of the nanocarbon on the electrode surface [16].

In this work, we demonstrate for the first time that 3DnCEs provide improved sensing of phenolic compounds through voltammetric measurements. In this case the oxidation process is promoted by delaying the kinetics of polymeric film formation [17] on the electrode surface, so it is possible to sense the analytes at a higher concentration than is possible with a glassy carbon electrode. Cyclic voltammetry (CV) and differential pulse voltammetry (DPV) techniques have been used to investigate the oxidation behavior of phenols. Furthermore, the pH conditions have been optimized to provide an enhanced electrochemical response to the phenolic compounds. 3DnCEs have been shown to be able to detect several compounds simultaneously. These developments provide an insight into the application of 3DnCEs for the voltammetric detection of phenolic compounds.

2. Experimental

2.1. Reagents

Phenol, 2,3-dichlorophenol, 2,4-dichlorophenol, 2,6-dichlorophenol, 3-chlorophenol, 4-chlorophenol, 2,4,6-trichlorophenol, and 4-nitrophenol were purchased from Sigma-Aldrich (Czech Republic). Monobasic potassium phosphate (Sigma) and dibasic potassium phosphate (Merck), sodium chloride (Merck) and potassium chloride (Merck) were used for the preparation of the phosphate buffer solution (PBS). Deionized water with a resistivity not less than 18.2 M Ω cm was used. A commercially available conductive nanocarbon/poly(lactic acid) (PLA) filament (Graphene Laboratories Ink., New York, USA) was used for 3D printing of the electrodes. pH values were measured with a Thermo Scientific Orion Star A111 pH meter.

2.2. Fabrication of 3DnCEs using graphene/PLA filaments

3DnCEs were fabricated using fused deposition modelling, a method in which a spool of thermoplastic filament is melted inside a printing nozzle and laid down layer by layer according to a pre-defined printer program (Prusa3 MK3s printer, Prusa Research, Czech Republic) using an Olsson Ruby ruby-tipped 0.6 mm nozzle (3DVerkstan, Sweden). The nanocarbon/PLA filament is extruded from the nozzle using a temperature of 220 °C and a bed temperature of around 60 °C [13,18,19]. The dimensions of the 3D-printed electrode are as follows: length: 1.6 cm, width: 0.6 cm ($r = 0.3$ cm) and thickness: 3 mm. The width of the rectangular part was 0.2 cm. The circular portion of the electrode was immersed in the electrolytic solution for the electrochemical measurements [20–22]. The electrochemically active area was calculated to be 1.86 cm². The resulting electrode consists of a composite of conductive graphene and non-conductive PLA polymer. To improve the electrical conductivity of the electrode, it was activated by immersion in the solvent DMF for six hours. After six hours, the electrodes were rinsed thoroughly with ethanol and then with ultrapure water and allowed to dry for 24 h [14].

2.3. Electrochemical instruments

The electrochemical measurements were conducted at room temperature (25 °C) using a three-electrode configuration, with Ag/AgCl (1 M KCl) as the reference electrode, a platinum wire as the counter electrode, and 3DnCE as the working electrode, using a Metrohm Autolab potentiometer (PGSTAT 204) operated by Nova 2.14 software.

2.4. Material characterization

The surface morphology of the 3DnCEs was examined by scanning

electron microscopy (SEM), using a Verios 460L instrument (FEI, USA), to compare the surface before and after DMF treatment.

2.5. Electrochemical detection

The influence of pH on the voltammograms of 4-chlorophenol was investigated by CV by using 50 μ M 4-chlorophenol in 100 mM PBS at different pH values (3, 5, 7, 9, 11) as an electrolyte solution. The same scan rate (10 mV s⁻¹) was used for the different analytes.

5 mM stock solutions of different phenols (2,3-dichlorophenol, 2,4-dichlorophenol, 2,6-dichlorophenol, 3-chlorophenol, 4-chlorophenol, 2,4,6-trichlorophenol, 4-nitrophenol) were prepared in 100 mM PBS solution and DPV was performed at pH 11 with different concentrations (25–125 μ M) of each analyte.

3. Results and discussion

As described previously, we activated the nanocarbon/PLA electrodes (3DnCEs) by immersion in DMF [16]. Structural characterization of 3DnCEs was performed using SEM to investigate the effect of the DMF treatment on the electrode morphology. The 3D-printed electrode surface is dominated by the presence of PLA, which aggregates with the nanocarbon to form a composite with a dense structure (Fig. 1A). The SEM image of the DMF-treated 3DnCEs (Fig. 1B) reveals that the PLA has been partly removed from the electrode surface, and that the nanocarbon has formed a mesh-like structure [14].

Subsequently, we employed the activated 3DnCE for detection of 4-chlorophenol as an archetypal compound. To evaluate the accuracy and precision of the 3DnCEs, five different electrodes have been studied in

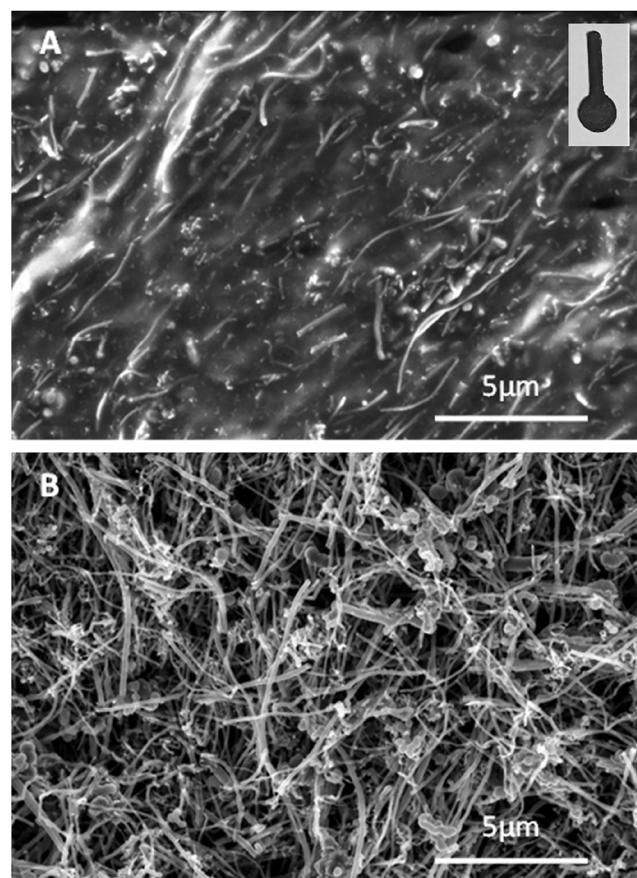


Fig. 1. SEM of 3DnCE (A) PLA/nanocarbon electrode without activation. The inset shows a photograph of the printed 3DnCE, circle diameter 0.6 cm (B) PLA/nanocarbon electrode after DMF activation.

100 μM 4-chlorophenol, as shown in Fig. S3. The output responses of all the different electrodes were consistent, providing a mean peak current at 0.24 μA and a relative standard deviation of 8.81% ($n = 5$). Since the pH plays a vital role in the electro-oxidation of 4-chlorophenol, as the phenolic group dissociates, the electrochemical characterization was carried out at various pH values. Cyclic voltammetry (Fig. 2A) shows the oxidation peak corresponding to the oxidation of 4-chlorophenol to the chloro-phenoxy radical, which appears during the positive scans. However, no reduction peak appears, suggesting that the process is chemically irreversible. Interestingly, reversible redox peaks at 0.3 V (oxidation) and 0.2 V (reduction) were observed at pH 3. This could be attributed to the presence of oxygenated functional groups (such as quinones) in the nanocarbon electrode [15]. When the pH is varied, the electrochemical behavior changes in two ways. As the pH increases, the peak intensity also increases significantly, but the oxidation of 4-chlorophenol is shifted to lower potential values. The rise in the peak intensity can be related to the availability of 4-chlorophenol in the anion form at higher pH values. Similarly, the shift of the peak towards lower potential values is related to the low pK_a value of the 4-chlorophenol, because on shifting from an acidic medium to alkaline solutions, the concentration of H^+ ions decreases, which shifts the equilibrium towards the 4-chlorophenol anion species (see Eq. (1)).



Fig. 2B shows oxidation potential values as a function of pH in PBS. The oxidation potential value decreases with the increase in pH values, following a linear trend, which is in close agreement with the Nernst equation (Eq. (2)):

$$E = E^0 + 0.059\text{pH} \quad (2)$$

where E^0 is the standard electrode potential, and E is the potential at 25 $^\circ\text{C}$. The slope extracted from the fitted equation ($y = -0.0487x + 1.0604$) is 0.0487, as shown in Fig. 2B, corresponding to approximately $n = 1$ from $0.059/n$. This implies that during the oxidation of 4-chlorophenol, one electron and one proton are transferred in an electrochemical reaction.

These results emphasize the influence of pH on the electro-oxidation of 4-chlorophenol and suggest that the oxidation reaction would be favored in a strongly alkaline medium (pH 11). The oxidation reaction is favored because the current obtained at that pH is the highest and the oxidation potential the lowest. Further studies were carried out using this optimum pH value.

The voltammetric behavior of 2,3-dichlorophenol, 2,4-dichlorophenol, 2,6-dichlorophenol, 3-chlorophenol, 4-chlorophenol, 2,4,6-trichlorophenol, 4-nitrophenol, and phenol was studied using differential pulse voltammetry (DPV). Fig. 3 displays the typical voltammograms of various chlorophenols, 4-nitrophenol, and phenol in PBS (100

mM, pH 11) using 3DnCE. Each of these phenolic compounds displays an oxidation peak, attributed to the formation of the corresponding phenolate ions, which appear at different potentials and provide different currents. These differences in electrochemical behavior can be correlated with the structural differences between the compounds.

It has been reported that the electrochemical oxidation of aromatic compounds may be influenced by the number of substituents, as well as their electronic nature and their position on the aromatic ring [23]. Ring substituents can influence the reactivity of phenolic compounds not only through steric, resonance (mesomeric, $\pm\text{M}$), and field (inductive, $\pm\text{I}$) effects, but electron-withdrawing substituents can also decrease the basicity (lower the pK_a) of phenol. On the other hand, electron-donating substituents can increase the basicity and nucleophilicity of phenol [24]. The pK_a values of phenol, 4-chlorophenol, 2,4-dichlorophenol, 3-chlorophenol, 2,6-dichlorophenol, 2,3-dichlorophenol, 2,4,6-trichlorophenol and 4-nitrophenol are 10.02, 9.38, 7.89, 9.02, 6.79, 7.45, 6.42, 7.15, respectively [25]. The corresponding oxidation potentials vs Ag/AgCl are 498 mV, 513 mV, 568 mV, 593 mV, 612 mV, 637 mV, 670 mV, 901 mV, respectively. There is an increase in the oxidation potential of disubstituted chlorophenols compared to monosubstituted chlorophenols. The greater stability of the compounds is directly correlated to the number of substituents which favor electronic delocalization, hence lowering the acidic strength of the compound [26]. Thus, phenolic compounds with electron-withdrawing substituents are more resistant to oxidation than phenols with electron-donating substituents.

Calibration curves were constructed for 3-chlorophenol, 4-nitrophenol, 4-chlorophenol, and phenol. Fig. 4(A–D) shows the DPV responses of the 3DnCEs using different concentrations of 3-chlorophenol, 4-nitrophenol, 4-chlorophenol, and phenol in 100 mM PBS at pH 11. Comparing the DPVs obtained in the presence and absence of analytes illustrates the successful electro-oxidation of the phenols, chlorophenols, and nitrophenol. These compounds show characteristic oxidation peaks using the 3DnCEs, and their intensity is proportional to the concentration. To compare the analytical performance of 3D-printed electrode with glassy carbon, a concentration calibration study of 4-nitrophenol was carried out (Figs. S1 and S2) using a glassy carbon electrode. Fig. S1 shows the DPV response of the glassy carbon electrode as the concentration of 4-nitrophenol is varied. Similarly, Fig. S2 shows the concentration calibration curve of 4-nitrophenol using a glassy carbon electrode. It is clear that after 100 μM concentration passivation of the electrode occurs, as there is a decrease in the current intensity at 125 μM compared to 100 μM . By contrast, Fig. 4(B) shows the same study carried out using a 3DnCE electrode, where no passivation is observed and the peak intensity increased continuously as far as 125 μM concentration. Furthermore, the current peak intensities of the glassy carbon electrode were lower than those of the 3DnCE. However, the peak potential is observed at 0.88 V, which is similar to the value found with the 3DnCE.

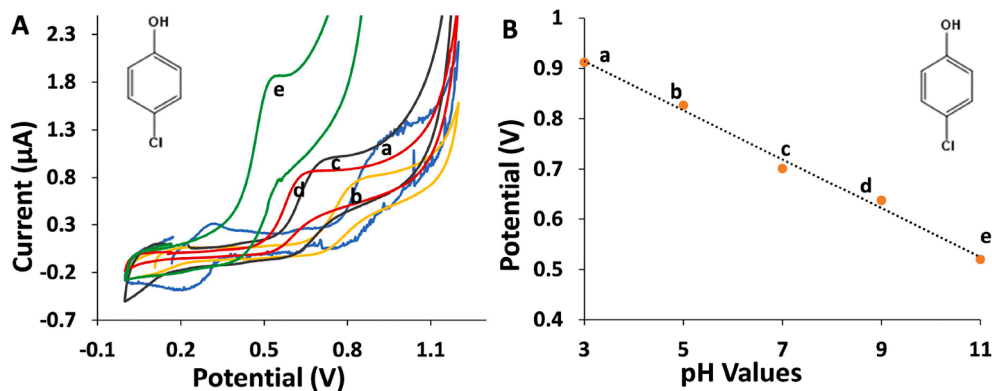


Fig. 2. (A) Influence of pH on CV response of 50 μM 4-chlorophenol in 100 mM PBS between +1.2 V and 0 V at a scan rate of 10 mVs^{-1} and (a) pH 3 (b) pH 5 (c) pH 7 (d) pH 9 (e) pH 11. (B) Oxidation potential values of 50 μM 4-chlorophenol as a function of pH in PBS.

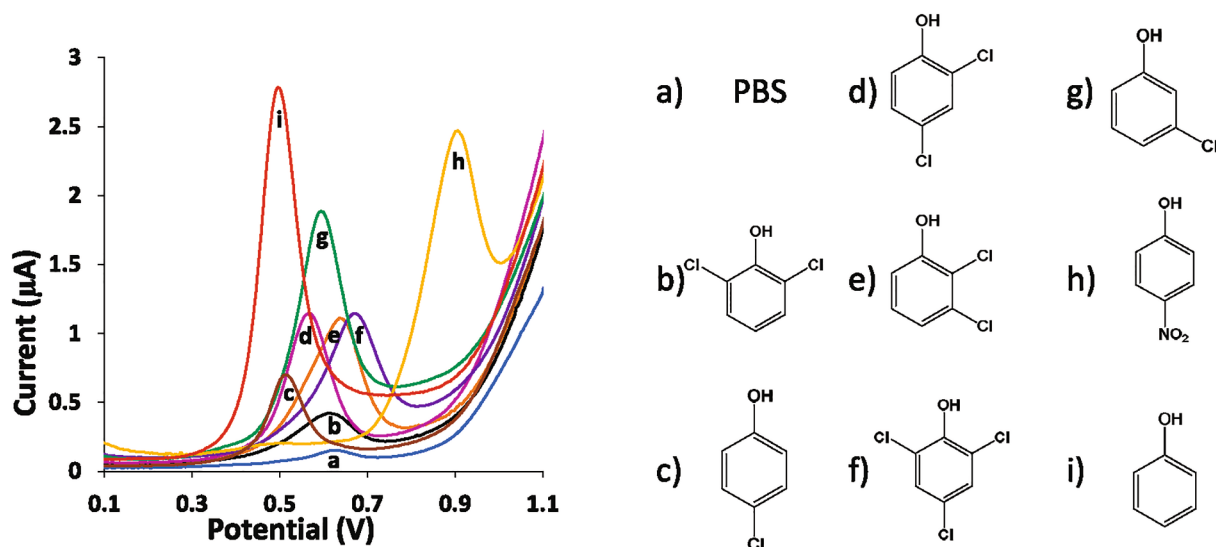


Fig. 3. Influence of the chemical structure of chlorophenols, nitrophenol and phenol on their voltammetric response (a) PBS (b) 2,6-dichlorophenol (c) 4-chlorophenol (d) 2,4-dichlorophenol (e) 2,3-dichlorophenol (f) 2,4,6-trichlorophenol (g) 3-chlorophenol (h) 4-nitrophenol (i) phenol, conc. 50 μM . Conditions: DPV scan rate 10 mV s^{-1} , PBS buffer (100 mM, pH 11).

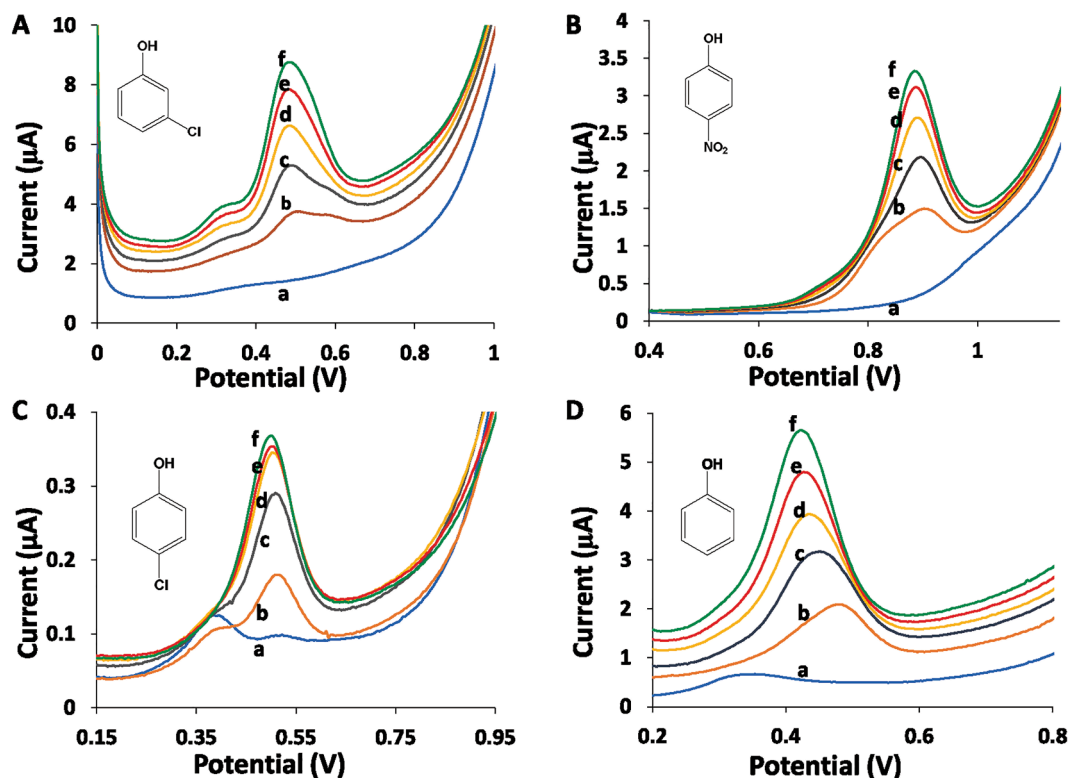


Fig. 4. Effect of concentration of (A) 3-chlorophenol (B) 4-nitrophenol (C) 4-chlorophenol and (D) phenol on the DPV response (a) in PBS, (b) 25 μM , (c) 50 μM , (d) 75 μM , (e) 100 μM and (f) 125 μM of each analyte, respectively, using 100 mM PBS at pH 11.

The calibration graphs of peak current density versus analyte concentration are plotted in Fig. 5 for different phenols, chlorophenols, and nitrophenols. Interestingly, the linear plots for all the analytes gave similar results, i.e., the peak current density increases with the increase in the concentration and reaches a maximum value at 125 μM . By comparison, the maximum concentration is lower with the glassy carbon electrode, only reaching 100 μM . Hence, the 3D-printed electrode shows a better response with lower rates of passivation compared to glassy carbon electrodes.

The calibration curves obtained for 3-chlorophenol, 4-nitrophenol, 4-chlorophenol, and phenol are $y = 0.0325x + 0.4257$, $y = 0.0165x + 0.3408$, $y = 0.0014x + 0.0917$ and $y = 0.0273x + 0.5152$, respectively. It is clear that detection of 4-chlorophenol and phenol is more sensitive than that of the remaining compounds [27].

We then investigated the simultaneous detection of phenols. Two simultaneous detections of mixtures 3-chlorophenol with 4-nitrophenol, and phenol with 4-nitrophenol were carried out by DPV analysis (Fig. 6) using 3DnCEs. This was performed simultaneously by keeping the same

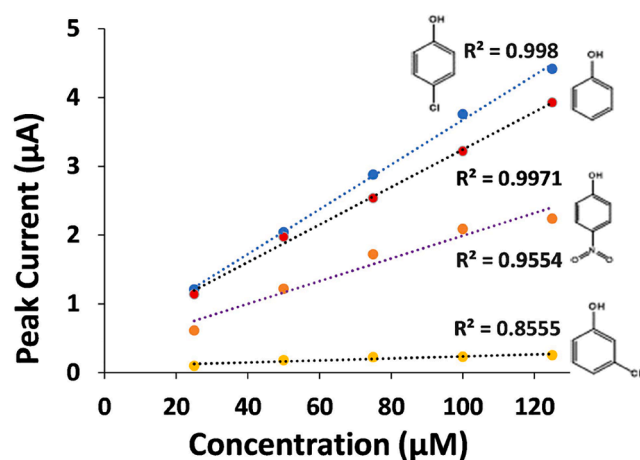


Fig. 5. DPV calibration curves of (a) 3-chlorophenol (b) 4-nitrophenol (c) 4-chlorophenol and (d) phenol in the concentration range 25–125 μM in 100 mM PBS at pH 11.

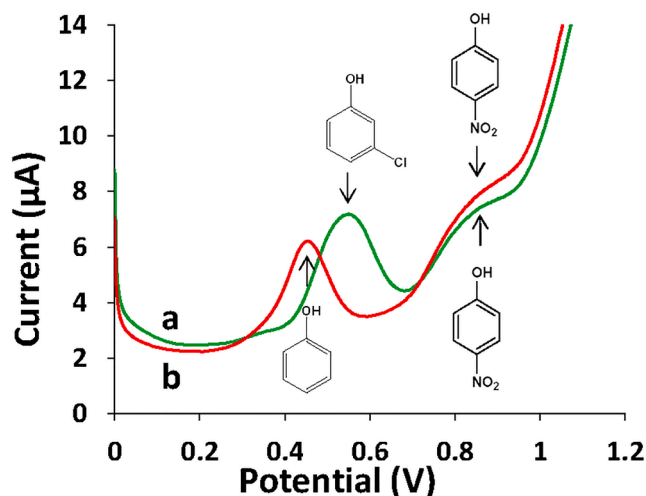


Fig. 6. Determination of mixtures of phenols. DPVs for mixtures of phenolic compounds in 100 mM PBS at pH 11: (a) 3-chlorophenol and 4-nitrophenol and (b) phenol and 4-nitrophenol at 50 μM concentrations of each compound.

concentration (50 μM) of each compound. The results show well-defined independent anodic peaks at 0.545 V and 0.823 V; and 0.450 V and 0.805 V, which correspond to the oxidation of 3-chlorophenol and 4-nitrophenol; or phenol and 4-nitrophenol, respectively. This indicates that the simultaneous determination of 3-chlorophenol and 4-nitrophenol, or phenol and 4-nitrophenol is possible using 3DnCEs [28].

4. Conclusion

We have demonstrated the utility of 3D-printed nanocarbon electrodes for the individual and simultaneous detection of phenolic compounds in aqueous solution. The electrochemical behavior of a range of phenolic compounds was thoroughly investigated using voltammetry. The influence of pH on the oxidation of phenols was studied and it was found that an alkaline pH is most suitable for the detection of these phenolic compounds. The chemical nature of the substituent(s) plays a vital role in the oxidation potential of these phenolic compounds due to their inductive and mesomeric effects. Furthermore, an increase in the number of substituents also shifted the oxidation potential towards more positive values. The simultaneous analysis of various phenolic compounds in a mixture was also successfully carried out. Thus, 3D-printed

electrodes offer great promise for the environmental screening and industrial monitoring of toxic phenolic compounds.

CRedit authorship contribution statement

Jyoti: Methodology, Writing - original draft. Edurne Redondo: Writing - review & editing, Supervision. Osamah Alduhaish: Discussions, Supervision. Martin Pumera: Conceptualization, Supervision.

Declaration of Competing Interest

The authors declare that they have no known competing financial interests or personal relationships that could have appeared to influence the work reported in this paper.

Acknowledgment

This work was supported by the Distinguished Scientist Fellowship Program (DSFP) of King Saud University, Riyadh, Saudi Arabia.

Appendix A. Supplementary data

Supplementary data to this article can be found online at <https://doi.org/10.1016/j.elecom.2021.106984>.

References

- [1] J. Wang, R. Deo, M. Musameh, Stable and sensitive electrochemical detection of phenolic compounds at carbon nanotube modified glassy carbon electrodes, *Electroanalysis* 15 (2003) 1830–1834, <https://doi.org/10.1002/elan.200302772>.
- [2] N. Rohaizad, C.C. Mayorga-Martinez, M. Fojtů, N.M. Latiff, M. Pumera, Two-dimensional materials in biomedical, biosensing and sensing applications, *Chem. Soc. Rev.* 50 (2021) 619–657, <https://doi.org/10.1039/D0CS00150C>.
- [3] G. Achilli, G. Piero Cellerino, G. Melzi d'Eril, S. Bird, Simultaneous determination of 27 phenols and herbicides in water by high-performance liquid chromatography with multi-electrode electrochemical detection, *J. Chromatogr. A* 697 (1995) 357–362, [https://doi.org/10.1016/0021-9673\(94\)00791-7](https://doi.org/10.1016/0021-9673(94)00791-7).
- [4] A. Hilmi, J.H.T. Luong, A.L. Nguyen, Applicability of capillary electrophoresis with amperometric detection to study degradation of chlorophenols in contaminated soil, *Environ. Sci. Technol.* 31 (1997) 1794–1800, <https://doi.org/10.1021/es9608914>.
- [5] M.A. Crespín, M. Gallego, M. Valcarcel, Solid-phase extraction method for the determination of free and conjugated phenol compounds in human urine, *J. Chromatogr., B: Anal. Technol. Biomed. Life Sci.* 773 (2002) 89–96, [https://doi.org/10.1016/S1570-0232\(02\)00012-0](https://doi.org/10.1016/S1570-0232(02)00012-0).
- [6] S. Singh, N. Kumar, M. Kumar, Jyoti, A. Agarwal, B. MizaiKoff, Electrochemical sensing and remediation of 4-nitrophenol using bio-synthesized copper oxide nanoparticles, *Chem. Eng. J.* 313 (2017) 283–292, <https://doi.org/10.1016/j.cej.2016.12.049>.
- [7] S. Singh, N. Kumar, V.K. Meena, C. Kranz, S. Mishra, Impedometric phenol sensing using graphenated electrochip, *Sens. Actuators, B* 237 (2016) 318–328, <https://doi.org/10.1016/j.snb.2016.06.079>.
- [8] C. Terashima, T.N. Rao, B.V. Sarada, D.A. Tryk, A. Fujishima, Electrochemical oxidation of chlorophenols at a boron-doped diamond electrode and their determination by high-performance liquid chromatography with amperometric detection, *Anal. Chem.* 74 (2002) 895–902, <https://doi.org/10.1021/ac010681w>.
- [9] J. Wang, M.S. Lin, In situ electrochemical renewal of glassy carbon electrodes, *Anal. Chem.* 60 (1988) 499–502, <https://doi.org/10.1021/ac00156a026>.
- [10] J. Wang, M.P. Chatrathi, A. Mulchandani, W. Chen, Capillary electrophoresis microchips for separation and detection of organophosphate nerve agents, *Anal. Chem.* 73 (2001) 1804–1808, <https://doi.org/10.1021/ac001424e>.
- [11] J. Muñoz, M. Pumera, Accounts in 3D-printed electrochemical sensors: towards monitoring of environmental pollutants, *ChemElectroChem* 7 (2020) 3404–3413, <https://doi.org/10.1002/celec.202000601>.
- [12] C.L. Manzanera Palenzuela, M. Pumera, (Bio)analytical chemistry enabled by 3D printing: Sensors and biosensors, *TRAC Trends Anal. Chem.* 103 (2018) 110–118, <https://doi.org/10.1016/j.trac.2018.03.016>.
- [13] A. Ambrosi, M. Pumera, 3D-printing technologies for electrochemical applications, *Chem. Soc. Rev.* 45 (2016) 2740–2755, <https://doi.org/10.1039/C5CS00714C>.
- [14] M.P. Browne, F. Novotný, Z. Sofer, M. Pumera, 3D printed graphene electrodes' electrochemical activation, *ACS Appl. Mater. Interfaces* 10 (2018) 40294–40301, <https://doi.org/10.1021/acsami.8b14701.10.1021/acsami.8b14701.s001>.
- [15] E. Redondo, S. Ng, J. Muñoz, M. Pumera, Tailoring capacitance of 3D-printed graphene electrodes by carbonisation temperature, *Nanoscale* 12 (2020) 19673–19680, <https://doi.org/10.1039/D0NR04864J>.
- [16] C.L. Manzanera Palenzuela, F. Novotný, P. Krupička, Z. Sofer, M. Pumera, 3D-printed graphene/poly(lactic acid) electrodes promise high sensitivity in

- electroanalysis, *Anal. Chem.* 90 (2018) 5753–5757, <https://doi.org/10.1021/acs.analchem.8b00083>.
- [17] C.L. Manzanares-Palenzuela, S. Hermanova, Z. Sofer, M. Pumera, Proteinase-sculptured 3D-printed graphene/polylactic acid electrodes as potential biosensing platforms: towards enzymatic modeling of 3D-printed structures, *Nanoscale* 11 (2019) 12124–12131, <https://doi.org/10.1039/c9nr02754h>.
- [18] R. Singh, H.K. Garg, Fused deposition modeling – a state of art review and future applications, *Ref. Mod. Mater. Sci. Mater. Eng.* (2016), <https://doi.org/10.1016/b978-0-12-803581-8.04037-6>.
- [19] S.C. Daminabo, S. Goel, S.A. Grammatikos, H.Y. Nezhad, V.K. Thakur, Fused deposition modeling-based additive manufacturing (3D printing): techniques for polymer material systems, *Mater. Today Chem.* 16 (2020) 100248, <https://doi.org/10.1016/j.mtchem.2020.100248>.
- [20] J. Muñoz, E. Redondo, M. Pumera, Bistable (supra)molecular switches on 3D-printed responsive interfaces with electrical readout, *ACS Appl. Mater. Interfaces* (2020), <https://doi.org/10.1021/acsami.0c14487>.
- [21] J. Muñoz, F. Céspedes, M. Baeza, Effect of carbon nanotubes purification on electroanalytical response of near-percolation amperometric nanocomposite sensors, *J. Electrochem. Soc.* 162 (2015) B217, <https://doi.org/10.1149/2.0531508jes>.
- [22] E. Redondo, J. Muñoz, M. Pumera, Green activation using reducing agents of carbon-based 3D printed electrodes: Turning good electrodes to great, *Carbon* 175 (2021) 413–419, <https://doi.org/10.1016/j.carbon.2021.01.107>.
- [23] M. Tian, S.S. Thind, J.S. Dondapati, X. Li, A. Chen, Electrochemical oxidation of 4-chlorophenol for wastewater treatment using highly active UV treated TiO₂ nanotubes, *Chemosphere* 209 (2018) 182–190, <https://doi.org/10.1016/j.chemosphere.2018.06.042>.
- [24] A. Pintar, J. Levec, Catalytic oxidation of aqueous p-chlorophenol and p-nitrophenol solutions, *Chem. Eng. Sci.* 49 (1994) 4391–4407, [https://doi.org/10.1016/S0009-2509\(05\)80029-6](https://doi.org/10.1016/S0009-2509(05)80029-6).
- [25] T. Hanai, K. Koizumi, T. Kinoshita, R. Arora, F. Ahmed, Prediction of pK(a) values of phenolic and nitrogen-containing compounds by computational chemical analysis compared to those measured by liquid chromatography, *J. Chromatogr. A* 762 (1997) 55–61, [https://doi.org/10.1016/S0021-9673\(96\)01009-6](https://doi.org/10.1016/S0021-9673(96)01009-6).
- [26] M.S. Ureta-Zañartu, P. Bustos, M.C. Diez, M.L. Mora, C. Gutiérrez, Electro-oxidation of chlorophenols at a gold electrode, *Electrochim. Acta* 46 (2001) 2545–2551, [https://doi.org/10.1016/S0013-4686\(01\)00448-0](https://doi.org/10.1016/S0013-4686(01)00448-0).
- [27] T.S. Cheng, M.Z.M. Nasir, A. Ambrosi, M. Pumera, 3D-printed metal electrodes for electrochemical detection of phenols, *Appl. Mater. Today* 9 (2017) 212–219, <https://doi.org/10.1016/j.apmt.2017.07.005>.
- [28] A.A. Ensafi, E. Heydari-Bafrooei, B. Rezaei, Simultaneous detection of hydroxylamine and phenol using p-aminophenol-modified carbon nanotube paste electrode, *Cuihua Xuebao/Chin. J. Catal.* 34 (2013) 1768–1775, [https://doi.org/10.1016/S1872-2067\(12\)60652-4](https://doi.org/10.1016/S1872-2067(12)60652-4).